

Valorisation of spent tire rubber as carbon adsorbents for Pb(II) and W(VI) recovery in the framework of a circular economy

M. Bernardo¹, D. Dores¹, N. Lapa¹, F. Pinto², I. Matos¹, M. Ventura¹, I. Fonseca¹

¹LAQV/REQUIMTE, Faculdade de Ciências e Tecnologia, Universidade Nova de Lisboa, 2829-516 Caparica, Portugal

² Unidade de Bioenergia (UB), Laboratório Nacional de Energia e Geologia (LNEG), Estrada do Paço do Lumiar, Ed. J, 1649-038 Lisboa, Portugal.

Corresponding author's email: maria.b@fct.unl.pt

Abstract

Spent tire rubber-derived chars and their corresponding H₃PO₄ and CO₂-activated chars were used as adsorbents in the recovery of Pb(II) ion and W(VI) oxyanion from synthetic solutions. The raw chars and activated chars were thoroughly characterized, being observed that H₃PO₄-activated chars presented lower surface areas than the raw chars and acidic surface chemistry, which affected the performance of these samples as adsorbents as they showed the lower removal rates of metallic ions probably because these samples presented a low content of exchangeable cations. On the other hand, CO₂-activated chars presented increased surface areas and increased mineral content (probably, rich in exchangeable cations) compared to the raw chars, which granted them higher uptake capacities for both Pb(II) (103-116 mg/g) and W(VI) (27-31 mg/g) ions. Also, CO₂-activated samples presented the higher kinetic constants for the adsorption process.

The results shown in this work allow concluding that the valorisation of spent tire rubber through pyrolysis and the subsequent activation of the obtained chars is an alternative and feasible option to obtain efficient recovery materials of critical metallic elements.

Keywords: Activation, adsorbents, spent tire rubber, carbon materials, critical elements, pyrolysis

1. Introduction

In 2020, around 75,000 tons of spent tires (ST) were generated in Portugal [1], while in the European Union this value reached 3.5 million tons in 2018 [2]. The disposal of ST represents a major environmental concern worldwide; thus, new solutions to valorise these wastes in the framework of the circular economy must be promoted [3].

Nowadays, most of the ST rubber is mechanically recycled or sent to energetic valorisation through combustion [2]. This process, although allowing the recovery of the energetic content of the rubber, it implies the loss of material as well as the emission of greenhouse gases and toxic compounds. Mechanical recycling corresponds to the reduction of spent rubber to granules of different particle sizes to be later incorporated into playground floors, running tracks, football fields, and civil engineering applications, among others. These uses fall short of what is desirable to a complete drain of the collected ST annually. Moreover, the problem remains at the end of life of these rubber products – how to manage the spent rubber? Or get worse – how to separate the rubber from the other material components. Therefore, recycling industries are focused on increasing the value of secondary raw materials derived from tires through innovative and sustainable pathways [3].

Chemical recycling by pyrolysis is one option for recovering value from ST rubber [4]. Pyrolysis is the thermal decomposition of ST rubber under an oxygen-free atmosphere. It generates intermediate products such as gas, oil, and char, offering the possibility of increasing the recycling rates in addition to obtaining products that can be incorporated into new value chains [4,5] The chars must be submitted to upgrading treatments to effectively increase the viability of ST pyrolysis plants. Those upgrading processes may consist of activation processes (with acids, bases and/or gases) at relatively high temperatures, allowing the char to be converted into carbon materials with interesting surface properties. This opens the window for a wide range of applications in different industries

[6,7]. Among the many applications of those carbons, their unique properties make them highly efficient as adsorbents of a wide range of compounds [6].

On the other hand, wastes of electric and electronic equipment (WEEEs) and waste batteries and accumulators (WBAs), constitute two types of rising problems in technological and modern societies [8,9]. Currently, around 10 million tons per year of WEEEs and WBAs are introduced in Europe [10,11]. Therefore, increasing the collection, treatment, and valorisation of WEEEs and WBAs is an urgent need. Nevertheless, not all these wastes are properly collected and recycled at the end of their lifetimes, increasing the risk of environmental contamination by hazardous substances. Additionally, the loss of WEEEs and WBAs represent a loss of resources with high economic value. Thus, the recovery of critical materials from WEEEs and WBAs, due to their economic importance, supply risk, and hazardousness, is a priority in the circular economy action plan and an environmental emerging issue. Among the different treatment steps of WEEEs and WBAs [12], chemical decomposition by leaching or chemical treatment for later recovery of the critical materials from effluent solutions is critical. This recovery can be accomplished through the adsorption of the metals of interest from the leachates by using efficient adsorbents.

In this context, the present work aims to study the valorisation of ST rubber through pyrolysis and activation/functionalisation into high added-value carbon materials to be subsequently used as adsorbents in the recovery of lead ions (Pb(II)) and tungsten oxyanions (W(VI)) from synthetic effluents. Lead is a common element used in batteries and other electric and electronic equipment [13,14], with demonstrated toxicity to the environment and human health [15]. Tungsten is considered by the European Commission as a critical raw material, due to its high economic importance and supply risk to Europe [16].

2. Experimental section

2.1 Samples of Spent Tyre (ST) Rubber

Two types of tire rubber were used as precursors: Sample A, which is a cryogenic recycled rubber from tires of light vehicles (particle size: 0.18 - 0.60 mm); Sample B, which is a mechanically recycled rubber obtained from a mixture of tires of light vehicles and heavy trucks (particle size: 0.6 - 0.8 mm). Both rubber samples were submitted to the following characterizations:

- i) Elemental analysis (C, H, N, and S) (Thermo Finnigan-CE Instruments Flash EA 1112 CHNS analyser);
- ii) Thermogravimetric analysis (TGA) (30-900 °C, 5 °C/min, argon flow (Setaram Labsys EVO);
- iii) Ash content by TGA (Setaram Labsys EVO), 30-900 °C, 5 °C/min, airflow;
- iv) Mineral content, based on the EN 15290 standard. The samples were digested (3 mL H₂O₂ 30% v/v + 8 mL HNO₃ 65% v/v + 2 mL HF 40% v/v) in a microwave station (Milestone Ethos 1600 Microwave Labstation) and neutralized (20 mL H₃BO₃ 4% w/v). The acidic solutions were analysed by inductively coupled plasma-atomic emission spectroscopy (ICP-AES) (Horiba Jobin-Yvon) for the quantification of several chemical elements.

2.2 Pyrolysis and Chars

The pyrolysis assays were carried out in a stirred batch reactor (Parr Instruments, Hastelloy C276) which was purged and pressurized to 0.6 MPa with nitrogen (N₂). A heating rate of 5 °C/min was applied until the desired reaction temperature of 405 °C had been reached, which was then held for 30 min. After cooling to room temperature, the resulting chars were submitted to sequential extractions with hexane and acetone to remove the pyrolysis oil and tars soaked in the chars. Finally, the chars were washed with water. The chars obtained from rubber samples A and B were named as CA and CB, respectively, and submitted to the following characterizations:

- i) Elemental analysis, TGA, and mineral content as described above;
- ii) Ash content according to ASTM D1762 standard (750° C for 6 h);
- iii) pH_{pzc} was determined by preparing solutions of 0.1 M NaCl with initial pH values between 2.00 and 12.00. The pH correction was performed with solutions of NaOH and HCl with concentrations between 0.01 and 1 M. A mass of 0.1 g of char was added to 20 mL of each 0.1 M NaCl solution. The mixtures were shaken in a roller-table device for 24 h. pH_{pzc} corresponds to the plateau of the curve pH_{final} vs pH_{initial};
- iv) X-ray powder diffraction (XRPD), in which the diffractograms were obtained by using a benchtop X-ray diffractometer (RIGAKU, model MiniFlex II), with a Cu X-ray tube (30 kV/15 mA) by continuous scanning from 15° to 80° (2 θ) with a step size of 0.01° (2 θ) and a scan speed of 2°/min. Tentative identification of XRD peaks by matching with ICDD database of XRD software was performed;

v) Fourier Transform Infrared Spectroscopy (FTIR) by the KBr disk method (Perkin-Elmer-Spectrum 1000 Spectrometer) in the 4000–400 cm^{-1} range under a resolution of 1 cm^{-1} ;

vi) N_2 adsorption-desorption isotherms at 77 K obtained in an ASAP 2010 Micromeritics equipment. The adsorption data were used to calculate the apparent surface area (A_{BET}) through the BET equation. The total pore volume (V_{total}) was determined by the amount of N_2 adsorbed at the relative pressure $p/p_0 = 0.95$. The micropore volume (V_{micro}) was evaluated by the t-plot method, and the mesopore volume (V_{meso}) was determined by the difference between V_{total} and V_{micro} . The samples were previously outgassed overnight, under vacuum, at 150 °C.

2.3 Activated chars

CA and CB chars were then activated with CO_2 (physical activation) and H_3PO_4 (chemical activation). Physical activation was performed in a quartz reactor placed in a custom-made electric vertical tube furnace at 800 °C (heating rate of 10 °C/min) for 6 h, under a CO_2 flow of 100 mL/min. The activated chars obtained were named CA- CO_2 and CB- CO_2 .

In the chemical activation process, the chars were first impregnated with H_3PO_4 under a mass ratio of 1:1, at 50 °C, for 5 h, and then dried at 130 °C; the impregnated chars were placed in a quartz reactor inside the furnace and activated at 500 °C (heating rate of 5 °C/min), for 2 h, under an N_2 flow of 150 mL/min. Finally, the obtained carbons were thoroughly washed with deionized water until stable pH. The samples obtained from the chemical activation of chars A and B were coded as CA- H_3PO_4 and CB- H_3PO_4 , respectively.

The activated chars were characterized for elemental analysis, ash content, TGA, XRPD, FTIR, pH_{PZC} , and N_2 adsorption-desorption isotherms at 77 K, as described above for raw chars.

2.4 Adsorption assays

A synthetic solution with an initial W(VI) concentration of 100 mg/L was prepared by diluting a standard Ammonium Tungstate $(\text{NH}_4)_2\text{WO}_4$ solution of 1000 mg/L (Scharlau) with deionised water. Pb(II) solution with an initial concentration of 100 mg/L was prepared through the dissolution of $\text{Pb}(\text{NO}_3)_2$ salt (Merck) with deionised water.

Batch adsorption experiments were performed in 20 mL vials, at room temperature, under constant agitation in a multi-point stirrer. After each adsorption assay, the samples were filtered through vacuum by using 0.22 μm MCE membranes. The filtrates were analysed by ICP-AES for W(VI) and Pb(II) quantification. Duplicates were made for each assay.

The effect of pH on metal ion removal was evaluated for a pH range of 2-5 for Pb(II) and 2-7 for W(VI). These assays were performed with an adsorbent mass of 30 mg and 10 mL of solution with a metal concentration of 100 mg/L, and agitation for 24 h. The effect of contact time in the uptake capacity (kinetic study) of adsorbents was performed up to 72 h, at pH of 5 for Pb(II) and at pH of 2 for W(VI), with an adsorbent mass of 10 mg and 10 mL of solution, with a metal ion concentration of 100 mg/L. The influence of different initial concentrations (equilibrium studies) was performed at a contact time of 48 h, an adsorbent mass of 10 mg and 10 mL of solution with a metal ion concentration ranging from 20 to 200 mg/L for both metal ions.

W(VI) and Pb(II) removal efficiencies, R (%), and adsorbent uptake capacity, q_t (mg/g), were calculated by Eqs. 1 and 2, respectively:

$$R (\%) = \frac{(C_0 - C_f) \times 100}{C_0} \quad (1)$$

$$q_t = \frac{(C_0 - C_f) \times V}{m} \quad (2)$$

where C_0 and C_f are the initial and final concentrations (mg/L) of the metal ions, respectively, V (L) is the volume of solution, and m (g) is the adsorbent mass.

3. Results and discussion

3.1 Samples characterization

The yields of pyrolysis chars A (CA) and B (CB) after solvents extraction were 47.1 % wt. and 51.8 % wt, respectively. This result shows that a substantial amount of pyrolysis oil and tars rich in aromatic, cyclic, and aliphatic hydrocarbons can be removed and recovered from the chars [5,17].

The results from the characterizations performed on the rubber samples, chars, and activated chars are presented in Table 1. It can be observed that although both rubbers have similar CHNS compositions, their ash content is rather different, being the rubber A from light vehicle tires richer in inorganic matter.

The pyrolysis chars (CA and CB) presented a higher ash content than the rubbers, resulting from the concentration effect of the pyrolysis process. Also, the sulphur content increased in the produced chars, indicating that this element has a low volatilization degree at the pyrolysis temperature used in the present work and being retained in the carbon matrix [18]. These chars presented neutral pH_{PZC} values and their composition is in agreement with previous studies of rubber tire-derived chars [5,18,19].

The carbons resulting from H_3PO_4 activation presented much smaller sulphur content compared to the raw chars, as well as low pH_{PZC} . Acidic activation and the extensive H_2O washing of the produced carbons may have promoted the removal of sulphide compounds. On the other hand, the low pH_{PZC} indicates the introduction of acidic groups on the carbons' matrix. Nevertheless, the ash content increased despite the intensive washing of the resulting carbons; non-soluble inorganic matter was retained on the resulting carbons. The carbons from CO_2 activation presented increased basicity, probably due to a mineral concentration effect, which is confirmed with the higher ash content. In this case, the sulphur content of the carbons was not reduced.

Table 1. Elemental analysis, ash content, and pH_{PZC} of rubber and carbon samples.

	C (%)	H (%)	N (%)	S (%)	Ashes (%)	pH_{PZC}
Rubber A	79.20	7.07	0.40	1.64	9.16	n.d.
Rubber B	83.39	7.60	0.40	2.04	3.92	n.d.
CA	71.33	0.71	0.28	2.51	21.4	7.4
CB	79.06	0.86	0.33	3.94	13.9	6.7
CA- H_3PO_4	69.00	0.52	0.20	0.42	23.8	3.0
CB- H_3PO_4	70.16	0.48	0.24	0.44	21.3	2.8
CA- CO_2	70.26	0.16	0.23	2.90	27.3	8.5
CB- CO_2	76.26	0.14	0.29	3.70	17.5	7.8

n.d. – not determined.

Table 2 shows the textural parameters of the carbon samples obtained from N_2 adsorption-desorption isotherms. The chars presented both low surface areas and total pore volumes, which are typical for this type of material [18,19]. After the activation with H_3PO_4 , there was a slight decrease in the surface area, possibly due to pore blocking with functional groups or some destruction of the porosity. The activation with CO_2 allowed a small increase in the surface area due to the gasification reactions, but the burn-off (carbon gasification conversion) was low (12.5–15.0%).

Table 2. Textural parameters of carbon samples obtained from N_2 adsorption-desorption isotherm.

	A_{BET} (m^2/g)	V_{total} (cm^3/g)	V_{micro} (cm^3/g)	V_{meso} (cm^3/g)
CA	73	0.13	0.01	0.12
CB	90	0.13	0.02	0.11
CA- H_3PO_4	48	0.11	0.004	0.11
CB- H_3PO_4	42	0.09	0.004	0.09
CA- CO_2	95	0.14	0.02	0.12
CB- CO_2	104	0.12	0.03	0.09

The mineral content of the rubber samples and raw chars was determined, and the results are presented in Table 3. Aluminum (Al), Cadmium (Cd), Potassium (K), Sodium (Na), Selenium (Se), Silicon (Si), and Tin (Sn) were not detected in the samples. Generally, all the minerals presented higher concentrations in the resulting chars compared to the rubbers, due to a concentration effect of pyrolysis. The concentrations of Zinc (Zn) stand out since zinc oxide (ZnO) is used in the vulcanization process of tire rubber [20]. Calcium (Ca) also showed high concentrations because is usually used as an additive in tire manufacturing. Other relevant metals are Iron (Fe), Magnesium (Mg), and Copper (Cu).

XRD analysis allowed identifying the main crystalline mineral phases in carbon samples (Fig 1). All samples presented a broad diffraction band between 15–30 °(2 θ) associated with an amorphous carbon structure. Raw chars presented typical diffractograms of ST derived chars [21,22], where peaks attributed to zinc sulphide (ZnS) in the form of sphalerite (β -ZnS) and wurtzite (α -ZnS), formed in the reaction of sulphur with the zinc oxide present in ST rubber during pyrolysis, can be identified [23,24]. The chars activated with CO₂ presented a similar XRD pattern compared to the raw chars, although some peaks become sharper, due to the phase transition of sphalerite to wurtzite [25]. The samples activated with H₃PO₄ present a distinctive diffractogram with the disappearance of zinc-derived peaks and the appearance of new peaks mainly associated with the silicophosphate (SiP₂O₇) phase due to the reaction of amorphous silica with H₃PO₄ [26]. Although silicon was not detected in the raw chars, probably it was present at low concentrations below the detection limit, or it was not solubilized in the acidic digestion for mineral content determination. The activation promoted the concentration of this element that reacted with the acid, producing a crystalline compound.

Table 3. Mineral content of rubber and raw char samples ($\bar{X} \pm \sigma, n = 2$)

Concentration (mg/g)	Rubber A	Rubber B	CA	CB
Zn	29.2±0.19	38.6±5.37	69.6±1.75	93.5±0.79
Ca	13.0±3.9	6.38±0.18	21.9±0.52	11.9±0.82
Fe	2.18±0.55	4.25±0.27	4.96±0.09	8.75±0.15
Mg	0.815±0.239	0.870±0.105	1.79±0.09	1.74±0.01
Cu	0.473±0.049	1.02±0.17	0.318±0.014	1.63±0.03
Pb	0.081±0.027	0.043±0.001	0.118±0.003	0.112±0.000
Ti	0.067±0.009	<0.004	<0.004	<0.004
Mn	0.029±0.008	0.025±0.002	0.052±0.006	0.059±0.006
Ba	0.202±0.02	<4x10 ⁻⁵	<4x10 ⁻⁵	<4x10 ⁻⁵
Cr	0.002±0.002	0.006±0.003	0.008±0.000	0.010±0.003
Ni	0.004±0.000	0.004±0.001	0.012±0.000	0.016±0.000
Mo	<4x10 ⁻⁴	<4x10 ⁻⁴	0.036±0.000	0.120±0.006

$\bar{X} \pm \sigma$: average \pm standard deviation; n : number of samples analysed.

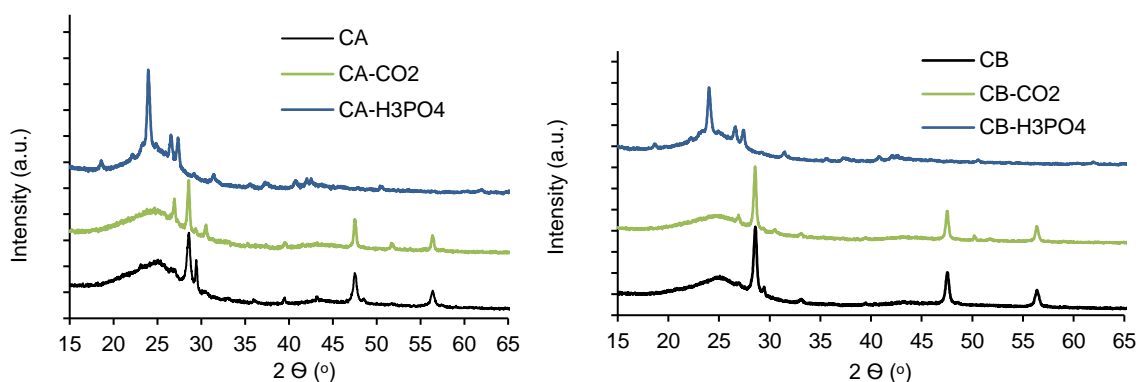


Fig. 1 XRD pattern of carbon samples (left: samples from rubber A; right: samples from rubber B)

Fig. 2 presents the FTIR spectra of carbon samples. Overall, the spectra are very similar with common bands at 3430 cm⁻¹ (stretching vibration of hydroxyl groups O-H of water), 2920 cm⁻¹ and 1384 cm⁻¹ (C-H stretching vibrations of methyl and methylene groups), 1630 cm⁻¹ (C=C or C=O stretch vibration), and in the range 900–750 cm⁻¹ (aromatic C-H out-of-plane bend) [22,27,28]. Also, all samples presented a strong band at 1100 cm⁻¹ that can be assigned to silicon-oxy compounds, Si–O–C or Si–O–Si, thus confirming the presence of silica [27]. Samples derived from H₃PO₄ activation presented a new and distinctive band at 1035 cm⁻¹ and a new group of small bands between 750–650 cm⁻¹ that can be associated with P–O–Si, Si–O–Si or P–O–P vibrations [29].

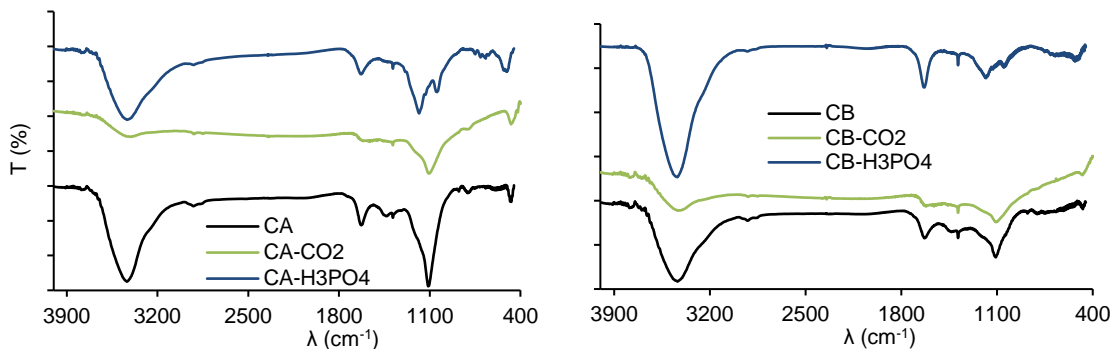


Fig. 2 FTIR spectra of carbon samples (left: samples from rubber A; right: samples from rubber B)

TGA analysis of rubber and carbon samples is presented in Fig. 3. Both ST rubbers A and B presented the main decomposition at a temperature range between 260–470 °C corresponding to a mass loss of around 60%, remaining 30 to 40% (w/w) of char product at 900 °C. The raw chars as well as the chars activated with CO₂ showed high thermal stability with a total mass loss below 10% (w/w). The activated chars with H₃PO₄ also presented thermal stability up to 750 °C. From this temperature onwards, they lose weight significantly up to 900 °C.

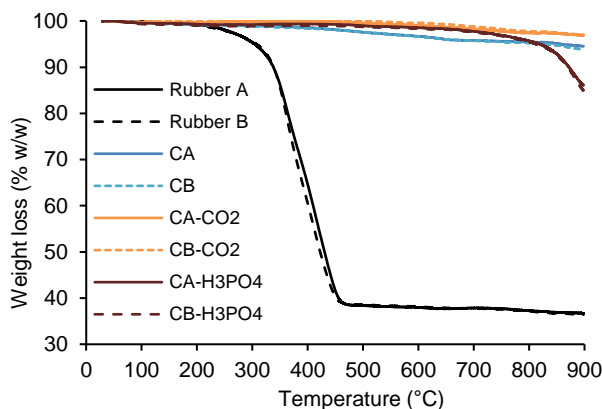


Fig. 3 TGA curves for ST rubbers and carbon samples.

3.2 Adsorption assays

The chars and activated chars were then applied as adsorbents of Pb(II) and W(VI) ions from aqueous solutions. The effect of pH on ions removal was evaluated for a pH range of 2–5 for Pb(II) and 2–7 for W(VI). The range of pH selected for Pb is related to the solubility of ion species, since Pb starts to precipitate as Pb(OH)₂ for alkaline conditions. Being an oxyanion, positively charged surfaces increase tungstate adsorption, therefore it was not worth it to study pH values above the pHPZC of carbon samples.

The higher removals of Pb(II) and W(VI) ions were obtained for initial pH values of 5 and 2, respectively. Almost 100% removal was achieved with the raw chars and CO₂-activated carbons for both metallic ions. Regarding Pb, the pH value of 5 corresponds to the natural pH of the Pb solution, and the lower removals for acidic conditions should be related to the higher concentration of H⁺ protons that compete with Pb²⁺ ions for the active sites of the carbons. Considering the significant content of metallic cations in both chars (Table 3), cation exchange is a presumable mechanism for Pb(II) adsorption [30]. For W(VI) ions, the higher removal rates were achieved for severe acidic conditions, since the carbons' surface is strongly protonated with positive charges and can electrostatically attract W(VI) oxyanions that can have negative valences (up to -7) under acidic conditions [31]. Carbons obtained from H₃PO₄ activation presented the lower removals, which can be related to their surface chemistry and/or textural properties since these samples have the lower surface areas (Table 2). Although these carbons have high mineral content (Table 1), the exchangeability of some of the metallic elements present in the raw chars may have decreased after the activation process.

According to these results, only the raw chars and activated chars with CO₂ were selected to be used in the next assays.

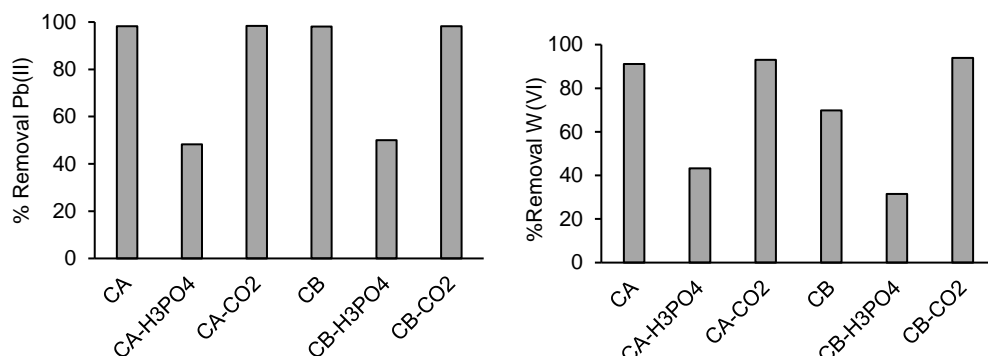


Fig. 4 Removal (%) of Pb(II) (left) and W(VI) (right) ions at initial pH of 5 and 2, respectively.

Conditions: adsorbent mass = 30 mg; Initial concentration of metal ions = 100 mg/L; solution volume = 10 mL; contact time = 24 h.

The results from the kinetic assays of Pb (II) and W(VI) adsorption are shown in Figs. 5 and 6, respectively. The experimental data was adjusted to both pseudo 1st order and pseudo 2nd order non-linear kinetic models [32,33] by using the minimum of the least-squares method with the SOLVER add-in of MS EXCEL. The best-fitting model, defined by the higher determination coefficient (R^2), for the kinetic data of both ions for all the adsorbents was the pseudo 2nd order model. Table 4 shows the kinetic parameters obtained from the modelling of experimental kinetic data to the pseudo 2nd order model.

Table 4. Kinetic parameters obtained from pseudo 2nd order kinetic modelling of Pb(II) and W(VI).

	Pb(II)			W(VI)		
	q_e (mg/g)	k_2 (g/mg.min)	R^2	q_e (mg/g)	k_2 (g/mg.min)	R^2
CA	43.0	0.004	0.967	33.1	0.001	0.932
CA-CO2	68.8	0.031	0.897	27.9	0.548	0.937
CB	62.9	0.002	0.934	12.4	0.03	0.986
CB-CO2	93.6	0.013	0.603	28.6	0.286	0.776

Overall, it is possible to conclude that the samples from CO₂ activation presented higher uptake capacities at equilibrium than the raw chars, which can be explained by the higher surface area of the activated samples (Table 2) and their higher ash content (Table 1). Thus, these samples are richer in cations able to exchange with Pb and W ions. Also, the kinetic constants obtained for the assays with the activated chars are the highest, being this fact quite evident for W(VI) adsorption. It should be highlighted the weaker adjustment of the kinetic model to the experimental data of the CB-CO2 sample, which can be indicative that a different kinetic model should be applied, as the adsorption mechanism is more complex. Also, the heterogeneity of the sample, revealed by relatively high error bars in the experimental points, can explain the weak adjustment of the theoretical model. Generally, all the samples achieved adsorption equilibrium for the two ions around 48 h.

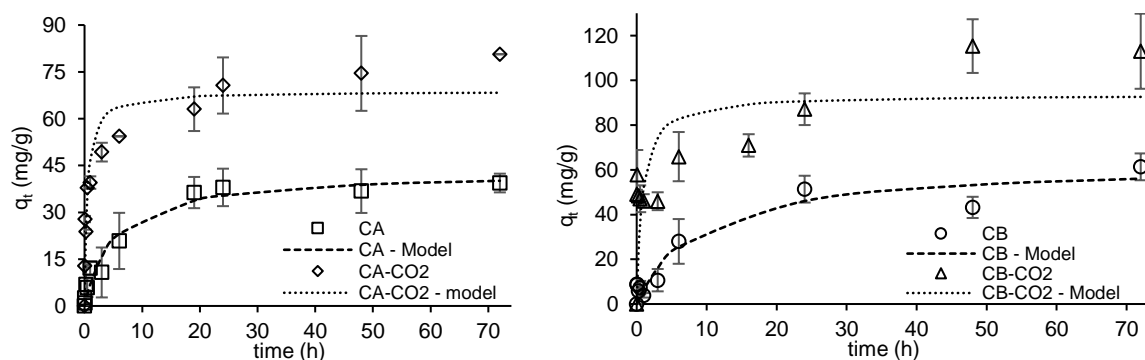


Fig. 5 Kinetic data of Pb(II) ions adsorption adjusted to pseudo 2nd order kinetic model. Conditions: adsorbent mass = 10 mg; Pb(II) initial concentration = 100 mg/L; solution volume = 10 mL; initial pH = 5.

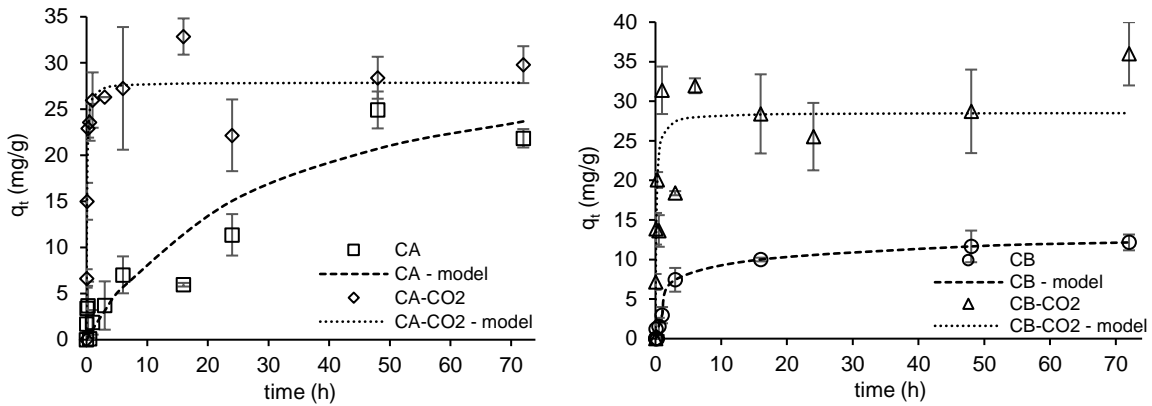


Fig. 6 Kinetic data of W(VI) ions adsorption adjusted to pseudo 2nd order kinetic model. Conditions: adsorbent mass = 10 mg; W(VI) initial concentration = 100 mg/L; solution volume = 10 mL; initial pH = 2.

Pb(II) and W(VI) adsorption isotherms are presented in Figs. 7 and 8, respectively. The experimental data were fitted to Langmuir and Freundlich non-linear models [34,35], by using also the minimum of the least-square method with the SOLVER tool. The obtained parameters are presented in Table 5 and the theoretical curves obtained with the best fitting model (Langmuir model) are also presented in Figs. 7 and 8.

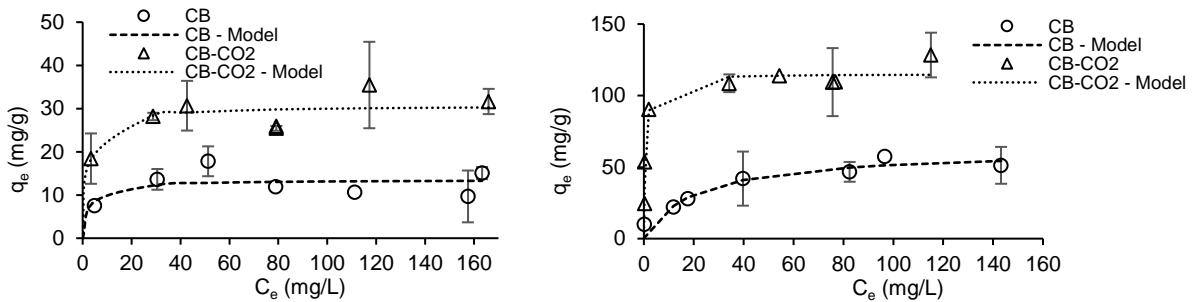


Fig. 7 Pb(II) adsorption isotherms adjusted to Langmuir model. Conditions: adsorbent mass = 10 mg; contact time = 48 h; solution volume = 10 mL; initial pH = 5

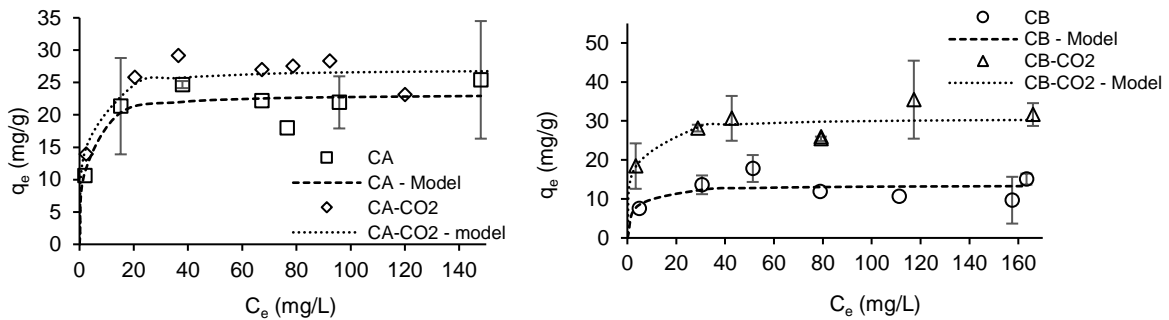


Fig. 8 W(VI) adsorption isotherms data adjusted to Langmuir model. Conditions: adsorbent mass = 10 mg; contact time = 48 h; solution volume = 10 mL; initial pH = 2

Table 5. Langmuir and Freundlich parameters obtained from modelling of experimental adsorption isotherm data of Pb(II) and W(VI) equilibrium studies.

		Pb(II)				W(VI)			
		CA	CA-CO2	CB	CB-CO2	CA	CA-CO2	CB	CB-CO2
<i>Langmuir</i>	q_m (mg/g)	39.1	103	62.1	116	23.3	27.1	13.5	30.7
	K_L (L/mg)	1.31	2.06	0.049	1.77	0.461	0.508	0.346	0.430
	R^2	0.978	0.899	0.961	0.955	0.930	0.936	0.749	0.921
<i>Freundlich</i>	K_F (mg/g)(mg/L) ⁿ	21.3	52.8	12.4	60.5	12.4	16.7	9.10	16.9
	n (dimensionless)	7.46	5.71	3.26	6.41	7.35	9.26	13.3	7.81
	R^2	0.911	0.821	0.959	0.915	0.884	0.855	0.689	0.921

The results confirm the best performance of CO₂-activated chars, showing the highest maximum uptake capacities of Pb (103–116 mg/g) and W (27–31 mg/g). Also, these carbon samples presented higher Langmuir constants (K_L) indicating a higher affinity for the ions.

Previous studies with tire-derived chars and activated chars applied as adsorbents of Pb(II) ions did not achieve such high uptake capacities [36–39]. Besides ion exchange, surface complexation and surface precipitation are also reasonable mechanisms to explain Pb(II) adsorption with these adsorbents, thus analyses of the loaded carbon samples and evaluations of the released cations after the adsorption assays are being envisaged.

Concerning W(VI), no studies on tungsten ion adsorption performed by chars or carbons were reported in the literature, apart from the work of Dias *et al.* [40], where the authors tested rice waste-derived porous carbons as highly efficient adsorbents of W(VI) oxyanions. Those authors also reviewed other adsorbents used for tungsten ions removal from aqueous solutions, and the uptake capacities of the char samples used in the present work are similar or even higher than many of those adsorbents.

4. Conclusions

ST rubber-derived chars and their corresponding H₃PO₄ and CO₂ activated samples were applied as adsorbents in the recovery of Pb(II) ion and (W(VI)) oxyanion from synthetic solutions. The carbon samples were extensively characterized, and it was observed that the H₃PO₄ activated chars presented lower surface areas than the raw chars and acidic surface chemistry which affected the performance of these samples as adsorbents since they presented the lower removal rates of the metal ions. It was also assumed that these carbon samples presented a low content of exchangeable cations. On the other hand, CO₂-activated chars presented increased surface areas and increased mineral content (probably rich in exchangeable cations) compared to the raw chars, which conferred them higher uptake capacities for both Pb(II) and W(VI) ions. Also, the CO₂ samples presented the higher kinetic constants of the adsorption process.

The results presented in this work allow concluding that the valorisation of spent tire rubber through pyrolysis and the subsequent activation of the obtained chars is an alternative option to obtain efficient recovery adsorbents of critical metallic elements.

Acknowledgments

The authors thank Valorpneu for the “Inov.Ação 2018” award. This work was also supported by the Associate Laboratory for Green Chemistry - LAQV which is financed by national funds from FCT/MCTES (UIDB/50006/2020 and UIDP/50006/2020).

References

- [1] Valorpneu, Newsletter Mensal, 2021. <https://mailchi.mp/fdef783b784e/e-valorpneu-n-1-novembro-5249234?e=ca62bdd2e1> (accessed May 27, 2021).
- [2] ERTMA, ELT Management Figures 2018, 2020. <https://www.etrma.org/wp-content/uploads/2020/09/Copy-of-ELT-Data-2018-002.pdf> (accessed May 27, 2021).
- [3] J. Araujo-Morera, R. Verdejo, M.A. López-Manchado, M. Hernández Santana, Sustainable mobility: The route of tires through the circular economy model, *Waste Manag.* 126 (2021) 309–322. doi:10.1016/j.wasman.2021.03.025.
- [4] R.G. dos Santos, C.L. Rocha, F.L.S. Felipe, F.T. Cezario, P.J. Correia, S. Rezaei-Gomari, Tire waste management: an overview from chemical compounding to the pyrolysis-derived fuels, *J. Mater. Cycles Waste Manag.* (2020). doi:10.1007/s10163-020-00986-8.
- [5] P.T. Williams, Pyrolysis of waste tyres: A review, *Waste Manag.* 33 (2013) 1714–1728. doi:10.1016/j.wasman.2013.05.003.
- [6] T.A. Saleh, V.K. Gupta, Processing methods, characteristics and adsorption behavior of tire derived carbons: A review, *Adv. Colloid Interface Sci.* 211 (2014) 93–101. doi:10.1016/j.cis.2014.06.006.
- [7] N. Antoniou, G. Stavropoulos, A. Zabaniotou, Activation of end of life tyres pyrolytic char for enhancing viability of pyrolysis – Critical review, analysis and recommendations for a hybrid dual system, *Renew. Sustain. Energy Rev.* 39 (2014) 1053–1073. doi:10.1016/j.rser.2014.07.143.
- [8] O.S. Shittu, I.D. Williams, P.J. Shaw, Global E-waste management: Can WEEE make a difference? A review of e-waste trends, legislation, contemporary issues and future challenges, *Waste Manag.* 120 (2021) 549–563. doi:10.1016/j.wasman.2020.10.016.
- [9] A.R. Dehghani-Sanij, E. Tharumalingam, M.B. Dusseault, R. Fraser, Study of energy storage systems and environmental challenges of batteries, *Renew. Sustain. Energy Rev.* 104 (2019) 192–208. doi:10.1016/j.rser.2019.01.023.
- [10] European Commission, Batteries and accumulators, (2021). https://ec.europa.eu/environment/topics/waste-and-recycling/batteries-and-accumulators_en (accessed May 27, 2021).
- [11] European Commission, Waste from Electrical and Electronic Equipment (WEEE), (2021). https://ec.europa.eu/environment/topics/waste-and-recycling/waste-electrical-and-electronic-equipment-weee_en (accessed May 27, 2021).
- [12] M. Kaya, Recovery of metals and nonmetals from electronic waste by physical and chemical recycling processes, *Waste Manag.* 57 (2016) 64–90. doi:10.1016/j.wasman.2016.08.004.
- [13] M. Li, J. Liu, W. Han, Recycling and management of waste lead-acid batteries: A mini-review, *Waste Manag. Res. J. a Sustain. Circ. Econ.* 34 (2016) 298–306. doi:10.1177/0734242X16633773.
- [14] J. Hao, Y. Wang, Y. Wu, F. Guo, Metal recovery from waste printed circuit boards: A review for current status and perspectives, *Resour. Conserv. Recycl.* 157 (2020) 104787. doi:10.1016/j.resconrec.2020.104787.
- [15] E.S. Ravipati, N.N. Mahajan, S. Sharma, K. V Hatware, K. Patil, The toxicological effects of lead and its analytical trends: an update from 2000 to 2018, *Crit. Rev. Anal. Chem.* 51 (2021) 87–102. doi:10.1080/10408347.2019.1678381.
- [16] G.A. Blengini, C.E.L. Latunussa, U. Eynard, C. Torres de Matos, D. Wittmer, K. Georgitzikis, C. Pavel, S. Carrara, L. Mancini, M. Unguru, D. Blagoeva, F. Mathieux, D. Pennington, Study on the EU’s list of Critical Raw Materials (2020) Final Report, Brussels, Belgium., 2020. doi:10.2873/904613.
- [17] M. Bernardo, M. Gonçalves, N. Lapa, R. Barbosa, B. Mendes, F. Pinto, Characterization of chars produced in the co-pyrolysis of different wastes: Decontamination study, *J. Hazard. Mater.* 207–208 (2012) 28–35. doi:10.1016/j.jhazmat.2011.07.115.
- [18] J.D. Martínez, N. Puy, R. Murillo, T. García, M.V. Navarro, A.M. Mastral, Waste tyre pyrolysis – A review, *Renew. Sustain. Energy Rev.* 23 (2013) 179–213. doi:10.1016/j.rser.2013.02.038.
- [19] N. Antoniou, A. Zabaniotou, Features of an efficient and environmentally attractive used tyres pyrolysis with energy and material recovery, *Renew. Sustain. Energy Rev.* 20 (2013) 539–558. doi:10.1016/j.rser.2012.12.005.
- [20] A.Y. Coran, Vulcanization, in: *Sci. Technol. Rubber*, Elsevier, 2013: pp. 337–381. doi:10.1016/B978-0-12-394584-6.00007-8.
- [21] Y.R. Smith, D. Bhattacharyya, T. Willhard, M. Misra, Adsorption of aqueous rare earth elements using carbon black derived from recycled tires, *Chem. Eng. J.* 296 (2016) 102–111. doi:10.1016/j.cej.2016.03.082.
- [22] S. Seng-eiad, S. Jitkarnka, Untreated and HNO₃-treated pyrolysis char as catalysts for pyrolysis of waste tire: In-depth analysis of tire-derived products and char characterization, *J. Anal. Appl. Pyrolysis.* 122 (2016) 151–159. doi:10.1016/j.jaap.2016.10.004.
- [23] H.-Y. Lin, W.-C. Chen, C.-S. Yuan, C.-H. Hung, Surface Functional Characteristics (C, O, S) of Waste Tire-Derived Carbon Black before and after Steam Activation, *J. Air Waste Manage. Assoc.* 58 (2008)

- 78–84. doi:10.3155/1047-3289.58.1.78.
- [24] F.A. López, T.A. Centeno, O. Rodríguez, F.J. Alguacil, Preparation and characterization of activated carbon from the char produced in the thermolysis of granulated scrap tyres, *J. Air Waste Manage. Assoc.* 63 (2013) 534–544. doi:10.1080/10962247.2013.763870.
- [25] Y. Li, W. Tan, Y. Wu, Phase transition between sphalerite and wurtzite in ZnS optical ceramic materials, *J. Eur. Ceram. Soc.* 40 (2020) 2130–2140. doi:10.1016/j.jeurceramsoc.2019.12.045.
- [26] M. Khabbouchi, K. Hosni, M. Mezni, E. Srasra, Simplified synthesis of silicophosphate materials using an activated metakaolin as a natural source of active silica, *Appl. Clay Sci.* 158 (2018) 169–176. doi:10.1016/j.clay.2018.03.027.
- [27] J. Coates, Interpretation of Infrared Spectra, A Practical Approach, in: *Encycl. Anal. Chem.*, John Wiley & Sons, Ltd, Chichester, UK, 2006. doi:10.1002/9780470027318.a5606.
- [28] B. Acevedo, C. Barriocanal, Texture and surface chemistry of activated carbons obtained from tyre wastes, *Fuel Process. Technol.* 134 (2015) 275–283. doi:10.1016/j.fuproc.2015.02.009.
- [29] M. Khabbouchi, K. Hosni, M. Mezni, E. Srasra, Structural Characterizations and Mechanical Behavior of Activated Clay-Based Si₅(PO₄)₆O and SiP₂O₇ Compounds, *Silicon.* 12 (2020) 117–124. doi:10.1007/s12633-019-00218-1.
- [30] M. Bernardo, S. Mendes, N. Lapa, M. Gonçalves, B. Mendes, F. Pinto, H. Lopes, I. Fonseca, Removal of lead (Pb²⁺) from aqueous medium by using chars from co-pyrolysis, *J. Colloid Interface Sci.* 409 (2013) 158–165. doi:10.1016/j.jcis.2013.07.050.
- [31] B.J. Smith, V.A. Patrick, Quantitative Determination of Sodium Metatungstate Speciation by 183W N.M.R. Spectroscopy, *Aust. J. Chem.* 53 (2000) 965. doi:10.1071/CH00140.
- [32] S. Lagergren, About the theory of so-called adsorption of soluble substances, *Sven. Vetenskapsakad. Handlingar.* 24 (1898) 1–39.
- [33] Y. Ho, Review of second-order models for adsorption systems, *J. Hazard. Mater.* 136 (2006) 681–689. doi:10.1016/j.jhazmat.2005.12.043.
- [34] H. Freundlich, Über die Adsorption in Lösungen, *Zeitschrift Für Phys. Chemie.* 57U (1907). doi:10.1515/zpch-1907-5723.
- [35] I. Langmuir, The constitution and fundamental properties of solid and liquids II. Liquids., *J. Am. Chem. Soc.* 39 (1917) 1848–1906. doi:10.1021/ja02254a006.
- [36] L. Malise, H. Rutto, T. Seodigeng, L. Sibali, P. Ndiribw, Adsorption of Lead Ions onto Chemical Activated Carbon Derived From Waste Tire Pyrolysis Char: Equilibrium and Kinetics Studies, in: *Chem. Eng. Trans.*, 2020. doi:10.3303/CET2082071.
- [37] P. Lu, S. Tian-Yang, Z. Cui, Adsorption of Pb(II) by Activated Pyrolytic Char from Used Tire, in: *MATEC Web Conf.*, 2016. doi:10.1051/01009.
- [38] S. Ramola, T. Mishra, G. Rana, R.K. Srivastava, Characterization and pollutant removal efficiency of biochar derived from baggase, bamboo and tyre, *Environ. Monit. Assess.* 186 (2014) 9023–9039. doi:10.1007/s10661-014-4062-5.
- [39] R. Helleur, N. Popovic, M. Ikura, M. Stanciulescu, D. Liu, Characterization and potential applications of pyrolytic char from ablative pyrolysis of used tires, *J. Anal. Appl. Pyrolysis.* 58–59 (2001) 813–824. doi:10.1016/S0165-2370(00)00207-2.
- [40] D. Dias, D. Don, J. Jandosov, M. Bernardo, F. Pinto, I. Fonseca, A. Sanches, P.S. Caetano, S. Lyubchyk, N. Lapa, Highly efficient porous carbons for the removal of W(VI) oxyanion from wastewaters, *J. Hazard. Mater.* 412 (2021) 125201. doi:10.1016/j.jhazmat.2021.125201.